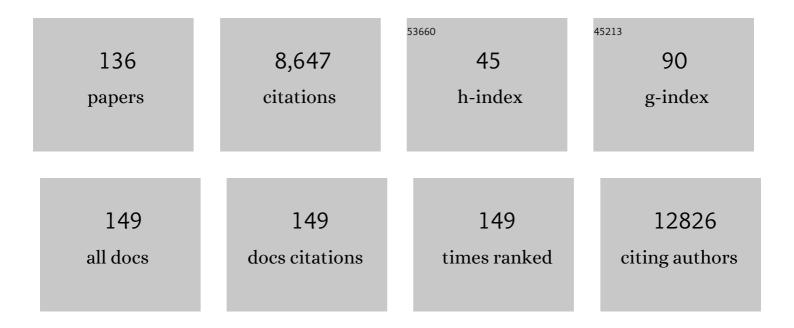
List of Publications by Year in descending order

Source: https://exaly.com/author-pdf/9375073/publications.pdf Version: 2024-02-01



HEINED EDIEDDICH

#	Article	IF	CITATIONS
1	The role of collagen in bone apatite formation in the presence of hydroxyapatite nucleation inhibitors. Nature Materials, 2010, 9, 1004-1009.	13.3	960
2	Towards stable catalysts by controlling collective properties of supported metal nanoparticles. Nature Materials, 2013, 12, 34-39.	13.3	606
3	Ion-association complexes unite classical and non-classical theories for the biomimetic nucleation of calcium phosphate. Nature Communications, 2013, 4, 1507.	5.8	602
4	3D printing of CNT- and graphene-based conductive polymer nanocomposites by fused deposition modeling. Applied Materials Today, 2017, 9, 21-28.	2.3	433
5	A chaotic self-oscillating sunlight-driven polymer actuator. Nature Communications, 2016, 7, 11975.	5.8	329
6	Zeoliteâ€Y Crystals with Trimodal Porosity as Ideal Hydrocracking Catalysts. Angewandte Chemie - International Edition, 2010, 49, 10074-10078.	7.2	265
7	Electron Tomography for Heterogeneous Catalysts and Related Nanostructured Materials. Chemical Reviews, 2009, 109, 1613-1629.	23.0	235
8	Imaging of Selfâ€Assembled Structures: Interpretation of TEM and Cryoâ€∓EM Images. Angewandte Chemie - International Edition, 2010, 49, 7850-7858.	7.2	202
9	Liquid–liquid phase separation during amphiphilic self-assembly. Nature Chemistry, 2019, 11, 320-328.	6.6	185
10	A classical view on nonclassical nucleation. Proceedings of the National Academy of Sciences of the United States of America, 2017, 114, E7882-E7890.	3.3	181
11	Design of supported cobalt catalysts with maximum activity for the Fischer–Tropsch synthesis. Journal of Catalysis, 2010, 270, 146-152.	3.1	170
12	Nucleation and Growth of Monodisperse Silica Nanoparticles. Nano Letters, 2014, 14, 1433-1438.	4.5	165
13	Molecular nucleation mechanisms and control strategies for crystal polymorph selection. Nature, 2018, 556, 89-94.	13.7	150
14	Conductive Screen Printing Inks by Gelation of Graphene Dispersions. Advanced Functional Materials, 2016, 26, 586-593.	7.8	139
15	Fractal parameters of individual soot particles determined using electron tomography: Implications for optical properties. Journal of Geophysical Research, 2007, 112, .	3.3	126
16	Mesoporous Silica Nanoparticles with Large Pores for the Encapsulation and Release of Proteins. ACS Applied Materials & Interfaces, 2016, 8, 32211-32219.	4.0	111
17	How nitric oxide affects the decomposition of supported nickel nitrate to arrive at highly dispersed catalysts. Journal of Catalysis, 2008, 260, 227-235.	3.1	103
18	Mesoporosity of Zeoliteâ€Y: Quantitative Threeâ€Dimensional Study by Image Analysis of Electron Tomograms. Angewandte Chemie - International Edition, 2012, 51, 4213-4217.	7.2	103

#	Article	IF	CITATIONS
19	Pt-Re synergy in aqueous-phase reforming of glycerol and the water–gas shift reaction. Journal of Catalysis, 2014, 311, 88-101.	3.1	103
20	Trained Immunity-Promoting Nanobiologic Therapy Suppresses Tumor Growth and Potentiates Checkpoint Inhibition. Cell, 2020, 183, 786-801.e19.	13.5	101
21	Microscopic structure of the polymer-induced liquid precursor for calcium carbonate. Nature Communications, 2018, 9, 2582.	5.8	100
22	Photoactivated nanomotors via aggregation induced emission for enhanced phototherapy. Nature Communications, 2021, 12, 2077.	5.8	97
23	Observation of a Ternary Nanocrystal Superlattice and Its Structural Characterization by Electron Tomography. Angewandte Chemie - International Edition, 2009, 48, 9655-9657.	7.2	95
24	Electron tomography of nanoparticle clusters: Implications for atmospheric lifetimes and radiative forcing of soot. Geophysical Research Letters, 2005, 32, .	1.5	94
25	Measuring Location, Size, Distribution, and Loading of NiO Crystallites in Individual SBA-15 Pores by Electron Tomography. Journal of the American Chemical Society, 2007, 129, 10249-10254.	6.6	94
26	Quantitative Structural Analysis of Binary Nanocrystal Superlattices by Electron Tomography. Nano Letters, 2009, 9, 2719-2724.	4.5	90
27	Mesoporous mordenites obtained by sequential acid and alkaline treatments – Catalysts for cumene production with enhanced accessibility. Journal of Catalysis, 2010, 276, 170-180.	3.1	90
28	Intermolecular channels direct crystal orientation in mineralized collagen. Nature Communications, 2020, 11, 5068.	5.8	90
29	Quantitative Characterization of Pore Corrugation in Ordered Mesoporous Materials Using Image Analysis of Electron Tomograms. Chemistry of Materials, 2009, 21, 1311-1317.	3.2	85
30	Heterogeneities of the Nanostructure of Platinum/Zeolite Y Catalysts Revealed by Electron Tomography. ACS Nano, 2013, 7, 3698-3705.	7.3	85
31	CryoTEM as an Advanced Analytical Tool for Materials Chemists. Accounts of Chemical Research, 2017, 50, 1495-1501.	7.6	82
32	Crystallization by particle attachment is a colloidal assembly process. Nature Materials, 2020, 19, 391-396.	13.3	78
33	Liquidâ€Phase Electron Microscopy for Soft Matter Science and Biology. Advanced Materials, 2020, 32, e2001582.	11.1	75
34	Three-Dimensional Structure of P3HT Assemblies in Organic Solvents Revealed by Cryo-TEM. Nano Letters, 2014, 14, 2033-2038.	4.5	74
35	Inkjet printing of graphene. Faraday Discussions, 2014, 173, 323-336.	1.6	70
36	Comparison of intensity distributions in tomograms from BF TEM, ADF STEM, HAADF STEM, and calculated tilt series. Ultramicroscopy, 2005, 106, 18-27.	0.8	66

#	Article	IF	CITATIONS
37	Quantitative Analysis of Electron Beam Damage in Organic Thin Films. Journal of Physical Chemistry C, 2017, 121, 10552-10561.	1.5	65
38	Enhancing the electrocatalytic activity of 2H-WS ₂ for hydrogen evolution <i>via</i> defect engineering. Physical Chemistry Chemical Physics, 2019, 21, 6071-6079.	1.3	60
39	Towards automated electron holographic tomography for 3D mapping of electrostatic potentials. Ultramicroscopy, 2010, 110, 390-399.	0.8	57
40	Controlling Internal Pore Sizes in Bicontinuous Polymeric Nanospheres. Angewandte Chemie - International Edition, 2015, 54, 2457-2461.	7.2	56
41	Hybrid Biodegradable Nanomotors through Compartmentalized Synthesis. Nano Letters, 2020, 20, 4472-4480.	4.5	56
42	Graphene-Flakes Printed Wideband Elliptical Dipole Antenna for Low-Cost Wireless Communications Applications. IEEE Antennas and Wireless Propagation Letters, 2017, 16, 1883-1886.	2.4	55
43	High-Resolution Electron Tomography Study of an Industrial Niâ^'Mo/γ-Al2O3Hydrotreating Catalyst. Journal of Physical Chemistry B, 2006, 110, 10209-10212.	1.2	49
44	Tunable Stimuliâ€Responsive Colorâ€Change Properties of Layered Organic Composites. Advanced Functional Materials, 2018, 28, 1804906.	7.8	48
45	The properties of SIRT, TVM, and DART for 3D imaging of tubular domains in nanocomposite thin-films and sections. Ultramicroscopy, 2014, 147, 137-148.	0.8	45
46	Unraveling the Role of Lithium in Enhancing the Hydrogen Evolution Activity of MoS ₂ : Intercalation versus Adsorption. ACS Energy Letters, 2019, 4, 1733-1740.	8.8	45
47	Controlling the Distribution of Supported Nanoparticles by Aqueous Synthesis. Chemistry of Materials, 2013, 25, 890-896.	3.2	44
48	Graphene screenâ€printed radioâ€frequency identification devices on flexible substrates. Physica Status Solidi - Rapid Research Letters, 2016, 10, 812-818.	1.2	44
49	Reversible Restructuring of Silver Particles during Ethylene Epoxidation. ACS Catalysis, 2018, 8, 11794-11800.	5.5	42
50	Conductivity Enhancement of Binderâ€Based Graphene Inks by Photonic Annealing and Subsequent Compression Rolling. Advanced Engineering Materials, 2016, 18, 1234-1239.	1.6	40
51	Polyhedral serpentine grains in CM chondrites. Meteoritics and Planetary Science, 2006, 41, 681-688.	0.7	36
52	Peptide nanotube formation: a crystal growth process. Soft Matter, 2012, 8, 7463.	1.2	36
53	Bicontinuous Nanospheres from Simple Amorphous Amphiphilic Diblock Copolymers. Macromolecules, 2013, 46, 9845-9848.	2.2	36
54	Liquid phase transmission electron microscopy with flow and temperature control. Journal of Materials Chemistry C, 2020, 8, 10781-10790.	2.7	35

#	Article	IF	CITATIONS
55	Periodic Mesoporous Organosilicas Consisting of 3D Hexagonally Ordered Interconnected Globular Pores. Journal of Physical Chemistry C, 2009, 113, 5556-5562.	1.5	34
56	Structure Sensitivity of Silver-Catalyzed Ethylene Epoxidation. ACS Catalysis, 2019, 9, 9829-9839.	5.5	34
57	Proteins as supramolecular hosts for C ₆₀ : a true solution of C ₆₀ in water. Nanoscale, 2018, 10, 9908-9916.	2.8	33
58	Writing Silica Structures in Liquid with Scanning Transmission Electron Microscopy. Small, 2015, 11, 585-590.	5.2	31
59	Tunable colloidal Ni nanoparticles confined and redistributed in mesoporous silica for CO ₂ methanation. Catalysis Science and Technology, 2019, 9, 2578-2591.	2.1	31
60	Gross morphological changes in thylakoid membrane structure are associated with photosystem I deletion in Synechocystis sp. PCC 6803. Biochimica Et Biophysica Acta - Biomembranes, 2012, 1818, 1427-1434.	1.4	30
61	Supramolecular Double Helices from Small C ₃ -Symmetrical Molecules Aggregated in Water. Journal of the American Chemical Society, 2020, 142, 17644-17652.	6.6	30
62	Understanding the effect of postsynthesis ammonium treatment on the catalytic activity of Au/Ti-SBA-15 catalysts for the oxidation of propene. Journal of Catalysis, 2008, 259, 43-53.	3.1	28
63	A Quantitative Electron Tomography Study of Ruthenium Particles on the Interior and Exterior Surfaces of Carbon Nanotubes. ChemSusChem, 2011, 4, 957-963.	3.6	28
64	Graphene oxide single sheets as substrates for high resolution cryoTEM. Soft Matter, 2015, 11, 1265-1270.	1.2	26
65	Native Chemical Ligation for Cross-Linking of Flower-Like Micelles. Biomacromolecules, 2018, 19, 3766-3775.	2.6	26
66	Multiscale Colloidal Assembly of Silica Nanoparticles into Microspheres with Tunable Mesopores. Advanced Functional Materials, 2020, 30, 2002725.	7.8	26
67	Visualizing order in dispersions and solid state morphology with Cryo-TEM and electron tomography: P3HT : PCBM organic solar cells. Journal of Materials Chemistry A, 2015, 3, 5031-5040.	5.2	23
68	Understanding the Formation Mechanism of Magnetic Mesocrystals with (Cryo-)Electron Microscopy. Chemistry of Materials, 2019, 31, 7320-7328.	3.2	22
69	Partial Oxidation as a Rational Approach to Kinetic Control in Bioinspired Magnetite Synthesis. Chemistry - A European Journal, 2015, 21, 6150-6156.	1.7	21
70	Establishing hierarchy: the chain of events leading to the formation of silicalite-1 nanosheets. Chemical Science, 2016, 7, 6506-6513.	3.7	21
71	Dynamics of silver particles during ethylene epoxidation. Applied Catalysis B: Environmental, 2020, 272, 118983.	10.8	21
72	Mapping and Controlling Liquid Layer Thickness in Liquidâ€Phase (Scanning) Transmission Electron Microscopy. Small Methods, 2021, 5, e2001287.	4.6	21

#	Article	IF	CITATIONS
73	A Robust Au/ZnCr ₂ O ₄ Catalyst with Highly Dispersed Gold Nanoparticles for Gas-Phase Selective Oxidation of Cyclohexanol to Cyclohexanone. ACS Catalysis, 2019, 9, 11104-11115.	5.5	20
74	A modular approach toward producing nanotherapeutics targeting the innate immune system. Science Advances, 2021, 7, .	4.7	20
75	2-Point correlation function of nanostructured materials via the grey-tone correlation function of electron tomograms: A three-dimensional structural analysis of ordered mesoporous silica. Acta Materialia, 2010, 58, 770-780.	3.8	19
76	On Packing, Connectivity, and Conductivity in Mesoscale Networks of Polydisperse Multiwalled Carbon Nanotubes. Journal of Physical Chemistry C, 2014, 118, 29796-29803.	1.5	19
77	The evolution of bicontinuous polymeric nanospheres in aqueous solution. Soft Matter, 2016, 12, 4113-4122.	1.2	19
78	Quantitative Analysis of Connectivity and Conductivity in Mesoscale Multiwalled Carbon Nanotube Networks in Polymer Composites. Journal of Physical Chemistry C, 2016, 120, 27618-27627.	1.5	19
79	Cryo-TEM and electron tomography reveal leaching-induced pore formation in ZSM-5 zeolite. Journal of Materials Chemistry A, 2019, 7, 1442-1446.	5.2	19
80	Spontaneous organization of supracolloids into three-dimensional structured materials. Nature Materials, 2021, 20, 541-547.	13.3	19
81	Isomeric periodic mesoporous organosilicas with controllable properties. Journal of Materials Chemistry, 2009, 19, 8839.	6.7	18
82	Photocatalytic activity of exfoliated graphite–TiO ₂ nanoparticle composites. Nanoscale, 2019, 11, 19301-19314.	2.8	18
83	Coiled coil driven membrane fusion between cyclodextrin vesicles and liposomes. Soft Matter, 2014, 10, 9746-9751.	1.2	16
84	Advanced tomography techniques for inorganic, organic, and biological materials. MRS Bulletin, 2016, 41, 516-521.	1.7	15
85	Quantitative nanoscopy: Tackling sampling limitations in (S)TEM imaging of polymers and composites. Ultramicroscopy, 2016, 160, 130-139.	0.8	15
86	ModifyingÂthe thickness, pore size, and composition of diatom frustule in Craspedostauros sp. with Al3+ ions. Scientific Reports, 2020, 10, 19498.	1.6	15
87	Biodegradable Elastic Sponge from Nanofibrous Biphasic Calcium Phosphate Ceramic as an Advanced Material for Regenerative Medicine. Advanced Functional Materials, 2021, 31, 2102911.	7.8	15
88	A simple and flexible route to large-area conductive transparent graphene thin-films. Synthetic Metals, 2015, 201, 67-75.	2.1	14
89	Quantification and optimization of ADF-STEM image contrast for beam-sensitive materials. Royal Society Open Science, 2018, 5, 171838.	1.1	14
90	Controlling Internal Pore Sizes in Bicontinuous Polymeric Nanospheres. Angewandte Chemie, 2015, 127, 2487-2491.	1.6	13

#	Article	IF	CITATIONS
91	Growth Kinetics of Cobalt Carbonate Nanoparticles Revealed by Liquid-Phase Scanning Transmission Electron Microscopy. Journal of Physical Chemistry C, 2019, 123, 25448-25455.	1.5	13
92	A Unified View on Nanoscale Packing, Connectivity, and Conductivity of CNT Networks. Advanced Functional Materials, 2019, 29, 1807901.	7.8	13
93	Studying Reaction Mechanisms in Solution Using a Distributed Electron Microscopy Method. ACS Nano, 2021, 15, 10296-10308.	7.3	13
94	H2PtCl6-derived Pt nanoparticles on USY zeolite: A qualitative and quantitative electron tomography study. Microporous and Mesoporous Materials, 2012, 164, 99-103.	2.2	11
95	On Resolution in Electron Tomography of Beam Sensitive Materials. Journal of Physical Chemistry C, 2014, 118, 1248-1257.	1.5	11
96	Bimodal Latex Effect on Spin-Coated Thin Conductive Polymer–Single-Walled Carbon Nanotube Layers. Langmuir, 2015, 31, 11982-11988.	1.6	11
97	Shearâ€Induced Orientation of Gyroid PSâ€ <i>b</i> â€P4VP(PDP) Supramolecules. Macromolecular Rapid Communications, 2013, 34, 1208-1212.	2.0	10
98	Counter-ion influence on the mechanism of HMTA-mediated ZnO formation. CrystEngComm, 2020, 22, 5854-5861.	1.3	10
99	Volume and surface-area measurements using tomography, with an example from the Brenham pallasite meteorite. Computers and Geosciences, 2008, 34, 1-7.	2.0	9
100	Low-dose (S)TEM elemental analysis of water and oxygen uptake in beam sensitive materials. Ultramicroscopy, 2020, 208, 112855.	0.8	9
101	Nanohybrid Materials with Tunable Birefringence via Cation Exchange in Polymer Films. Advanced Functional Materials, 2020, 30, 1907456.	7.8	9
102	Designing stable, hierarchical peptide fibers from block co-polypeptide sequences. Chemical Science, 2019, 10, 9001-9008.	3.7	8
103	The Influence and Removability of Colloidal Capping Agents on Carbon Monoxide Hydrogenation by Zirconia upported Rhodium Nanoparticles. ChemCatChem, 2017, 9, 1018-1024.	1.8	7
104	Time-Resolved Cryo-TEM Study on the Formation of Iron Hydroxides in a Collagen Matrix. ACS Biomaterials Science and Engineering, 2021, 7, 3123-3131.	2.6	7
105	Electron Holographic Tomography - Challenge and Opportunity. Microscopy and Microanalysis, 2004, 10, 1174-1175.	0.2	6
106	Biomimetic Mineralization of Calcium Phosphate on a Functionalized Porous Silicon Carbide Biomaterial. ChemPlusChem, 2012, 77, 694-699.	1.3	6
107	Characterization of hen phosvitin in aqueous salt solutions: Size, structure, and aggregation. Food Hydrocolloids, 2022, 129, 107545.	5.6	6
108	Controlled titration-based ZnO formation. CrystEngComm, 2021, 23, 3340-3348.	1.3	5

7

#	Article	IF	CITATIONS
109	Multiscale characterization of pathological bone tissue. Microscopy Research and Technique, 2022, 85, 469-486.	1.2	5
110	In Situ Manipulation and Micromechanical Characterization of Diatom Frustule Constituents Using Focused Ion Beam Scanning Electron Microscopy. Small Methods, 2021, 5, e2100638.	4.6	5
111	Chain length of bioinspired polyamines affects size and condensation of monodisperse silica particles. Communications Chemistry, 2021, 4, .	2.0	5
112	Hierarchical micro-/mesoporous zeolite microspheres prepared by colloidal assembly of zeolite nanoparticles. RSC Advances, 2020, 10, 36459-36466.	1.7	4
113	Building Reversible Nanoraspberries. Nano Letters, 2021, 21, 2232-2239.	4.5	4
114	Nanoscale chemical analysis of beamâ€sensitive polymeric materials by cryogenic electron microscopy. Journal of Polymer Science, 2021, 59, 1221-1231.	2.0	4
115	Crystallization via Oriented Attachment of Nanoclusters with Short-Range Order in Solution. Journal of Physical Chemistry C, 2021, 125, 1143-1149.	1.5	4
116	Local quantification of mesoporous silica microspheres using multiscale electron tomography and lattice Boltzmann simulations. Microporous and Mesoporous Materials, 2020, 302, 110243.	2.2	3
117	Correlative imaging for polymer science. Journal of Polymer Science, 2021, 59, 1232-1240.	2.0	3
118	The effects of washing a collagen sample prior to TEM examination. Microscopy Research and Technique, 2021, , .	1.2	3
119	Electron Holography of Nanomter-sized Magnetite Crystals. Microscopy and Microanalysis, 2003, 9, 174-175.	0.2	2
120	3D Nanoscale Analysis of Zeolite Catalysts by Electron Tomography and Image Processing. Microscopy and Microanalysis, 2014, 20, 784-785.	0.2	2
121	Time-resolved investigation of mesoporous silica microsphere formation using in situ heating optical microscopy. Journal of Colloid and Interface Science, 2021, 585, 118-125.	5.0	2
122	Electron Microscopy Techniques. , 2014, , 191-221.		2
123	Collagen mineralization with lepidocrocite <i>via</i> Fe(OH) ₂ addition. CrystEngComm, 2022, 24, 1211-1217.	1.3	2
124	Lipid Oxidation in Food Emulsions: Analytical Challenges and Recent Developments. , 2022, , 3-29.		2
125	In Situ Fabrication, Manipulation, and Mechanical Characterization of Free‣tanding Silica Thin Films Using Focused Ion Beam Scanning Electron Microscopy. Advanced Materials Interfaces, 2022, 9, .	1.9	2
126	Assembly of partially covered strawberry supracolloids in dilute and concentrate aqueous dispersions. Journal of Colloid and Interface Science, 2022, 627, 827-837.	5.0	2

#	Article	IF	CITATIONS
127	Liquid Phase Electron Microscopy of Soft Matter. Microscopy and Microanalysis, 2018, 24, 248-249.	0.2	1
128	Formation of Hierarchical Hybrid Silica-Polymer Using Quantitative Cryo- Electron Tomography. Microscopy and Microanalysis, 2019, 25, 59-60.	0.2	1
129	<i>In-Situ</i> Liquid Phase Electron Microscopy of Beam-Sensitive Materials. Microscopy and Microanalysis, 2019, 25, 63-64.	0.2	1
130	"No-dose―imaging. Microscopy and Microanalysis, 2021, 27, 2620-2622.	0.2	1
131	Binary Nanoparticle Superlattices in 3D: from Quantitative Analysis of Crystal Structures to Characterization of Lattice Defects Microscopy and Microanalysis, 2009, 15, 1192-1193.	0.2	0
132	Quantitative ET in Materials Chemistry. Microscopy and Microanalysis, 2018, 24, 1442-1443.	0.2	0
133	Towards Understanding the Mechanisms behind Templated Growth of 2D Magnetite Platelets via Bio-Inspired Approaches. Microscopy and Microanalysis, 2019, 25, 61-62.	0.2	0
134	Comment: Non-classical nucleation towards separation and recycling science: Iron and aluminium (Oxy)(hydr)oxides. Current Opinion in Colloid and Interface Science, 2020, 46, 128-129.	3.4	0
135	Mapping of oxygen and water related degradation across P3HT:PCBM interfaces. , 0, , .		0
136	Investigating the Morphology and Mechanics of Biogenic Hierarchical Materials at and below Micrometer Scale. Nanomaterials, 2022, 12, 1549.	1.9	0